

# Energy and exergy analysis of a photovoltaic-thermal system under two different climate conditions

*Sonja Kallio<sup>a</sup>, Monica Siroux<sup>b</sup>*

<sup>a</sup> INSA Strasbourg ICUBE, Strasbourg University, France, [sonja.kallio@insa-strasbourg.fr](mailto:sonja.kallio@insa-strasbourg.fr)

<sup>b</sup> INSA Strasbourg ICUBE, Strasbourg University, France, [monica.siroux@insa-strasbourg.fr](mailto:monica.siroux@insa-strasbourg.fr), CA

## Abstract:

Micro-cogeneration is a technology that generates simultaneously heat and electricity from a single fuel source for residential buildings. The micro-cogeneration systems are advantageous means of producing decentralized green energy and offer significant benefits: reduced primary energy consumption, reduced CO<sub>2</sub> emissions, avoidance of central plant and network construction. This paper proposes a dynamic model of a solar-based micro-cogeneration system called a photovoltaic-thermal (PVT) collector and relates to the energetic and exergetic analysis of the system under two different climate conditions. Energy and exergy analysis is undertaken to evaluate the performance of the PVT system. The exergy analysis is used to investigate the quality of the thermal and electrical energy produced by the PVT collector. Finally, a sensitivity analysis is conducted to understand the influence of the different parameters on the operation of the PVT system. Understanding the behaviour of the single PVT unit is the first step towards the optimization of the system under different climate conditions.

## Keywords:

Solar energy, renewable energy, micro-cogeneration, combined heat and power, energy analysis, exergy analysis

## 1. Introduction

Renewable energy production is getting a stronger role in energy production. Micro combined heat and power ( $\mu$ -CHP) generation systems are operating in the building sector to produce space heating, domestic hot water and electricity. The European Parliament has defined the micro-cogeneration to be the units up to an electrical output of 50 kW. Solar energy can be counted to be an inexhaustible source of energy and its use does not depend on the energy markets. The photovoltaic-thermal (PVT) collector is renewable solar-based micro-cogeneration unit which produces electricity by PV module and useful heat by cooling the PV module with coolant fluid circulation. This leads to increase overall system efficiency but also an increasing electrical efficiency due to decreased operation temperature of the PV module.

Different kind of PVT configurations has been developed and modelled in the literature. The collector can be, for example, air or water-based and its operation varies according to different parameters, such as geometry, thermo-physical properties and climate conditions (solar irradiation, wind speed and ambient temperature). The performance of the PVT system can be analysed based on the First Law of thermodynamics and the analysis can be extended to take into account the Second Law of thermodynamics. The thermodynamic analyses are called energy and exergy analyses. Compared to the energy analysis, the exergy analysis takes into account also the quality of the produced energy in terms of mechanical work.

The energy and exergy performance of the PVT collector is studied in [3, 5]. The dynamic simulation of the PVT combined with thermal storage is conducted and analysed in [4]. The climate conditions influence strongly on the performance of the PVT system. The energy performance of the PVT collector under two similar climate conditions is studied in [1]. In [5] the PVT performance in the five different cities in India is investigated. Three European cities Athens, London and Zaragoza are investigated as a location for the PVT system in [6].

This paper proposes a dynamic model of a PVT collector with a crystalline silicon roll-bond collector implemented in Matlab/Simulink. The weekly and yearly simulations of the collector are run under two different climate conditions in the northern Tampere, Finland and southern Strasbourg, France. The exergy performance analysis is conducted to see how efficient in reality the PVT operation is and if there is a difference between two different locations. Finally, a sensitivity analysis is conducted to understand the influence of the different parameters on the PVT collector operation.

## 2. Methods

### 2.1. Description of PVT

A water-based PVT collector with a direct flow geometry and roll bond channels is simulated and analysed in this study. Figure 1 shows the geometry and cross-section of the PVT collector [1]. The water-based PVT collector is investigated because they achieve higher overall efficiency than air-based collectors due to the higher heat capacity of water [2]. High efficient PV cells are still relatively expensive and in this study, the PVT collector has a crystalline silicon PV cell with a reference electrical efficiency ( $\eta_{STC}$ ) of 15% at the reference operating temperature ( $T_{ref}$ ) of 25°C. The temperature coefficient ( $\beta_T$ ) is 0.5%/K. The diameter of the tubes is 9 mm and the number is 10. The inlet temperature of the coolant fluid is 20 °C. Table 1 summarizes the main geometrical, thermo-physical, optical properties and the parameters of the PVT collector used in the simulation and analyses.

*Table 1. The main geometrical, thermo-physical and optical properties of the PVT collector. With \* the parameter varies with time.*

| Property                  | Glass | Air gap | PV    | Thermal absorber | Fluid | Insulation | Unit              |
|---------------------------|-------|---------|-------|------------------|-------|------------|-------------------|
| Emissivity ( $\epsilon$ ) | 0.9   | -       | 0.96  | -                | -     | -          | -                 |
| Absorbance ( $\alpha$ )   | 0.1   | -       | 0.9   | -                | -     | -          | -                 |
| Transmittance ( $\tau$ )  | 0.93  | -       | -     | -                | -     | -          | -                 |
| Thickness (H)             | 0.004 | 0.02    | 0.006 | 0.001            | -     | 0.04       | m                 |
| Area (A)                  | 2     | 2       | 2     | 2                | -     | 2          | m <sup>2</sup>    |
| Mass flow                 | -     | -       | -     | -                | 0.019 | -          | kg/s              |
| Density ( $\rho$ )        | 2200  | -       | 2330  | 2699             | 1050  | 16         | kg/m <sup>3</sup> |
| Specific heat (c)         | 670   | -       | 900   | 800              | 4180  | 1120       | J/(kgK)           |
| Conductivity (k)          | 1.1   | *       | 140   | 237              | 0.615 | 0.035      | W/(mK)            |

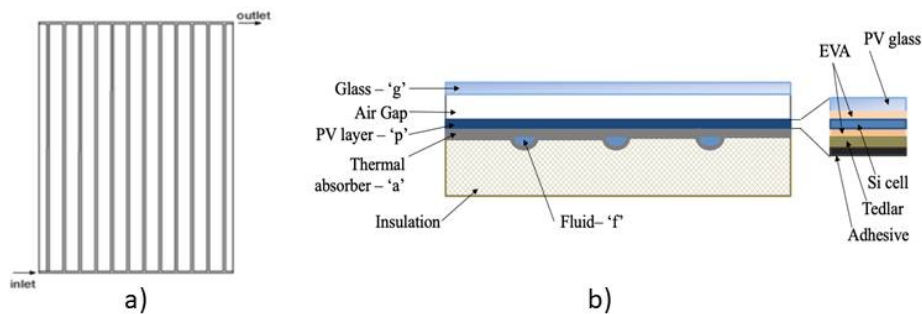


*Fig. 1. The PVT collector: a) Direct flow collector geometry; b) Cross section of the PVT collector*

In order to set up a simplified mathematical model of the PVT collector, it is assumed that the glass cover, air gap, PV cell and the absorber plate are one layer and the thermal resistance between them is negligible. From the layer there is heat transfer to the environment and coolant fluid. The

temperature distribution is uniform in the layer. It is also assumed that there are no heat losses through the edges; the optical and thermal properties of the materials and fluids are constant and no surrounding shading or dust is taken into account.

## 2.2. Meteorological data

The behaviour of the PVT collector depends strongly on the meteorological conditions. The main influencing weather parameters are the solar irradiation, ambient temperature and wind speed. The solar irradiation influences strongly on the electrical output of the PVT and it heats up the material layers of the collector through radiative heat transfer. The ambient temperature and wind speed influence on temperatures of the PVT layers through the convective and conductive heat transfer. The wind speed influences strongly on the heat losses through the surface and back of the PVT collector. In this paper, two different climate conditions are compared and the behaviour of the PVT collector under these conditions is investigated.

In this paper, the selected meteorological conditions are at Tampere, Finland and Strasbourg, France. Tampere is located in southern Finland in North Europe. Strasbourg is located in northern France at the border with Germany in Central Europe.

The hourly yearly meteorological data of Tampere was obtained from the experimental measuring centre of Tampere University. Similar data for Strasbourg was obtained from the Meteonorm Database.

The following Figs. present samples of the hourly climate data of Tampere and Strasbourg. Figure 2 shows the solar irradiation, ambient temperature and wind speed, respectively, during a summer week in Tampere and Strasbourg.

In Fig. 2a can be seen that during the summer period the solar irradiation in Tampere can reach the same maximum values around  $800 \text{ W/m}^2$  than in Strasbourg.

Figure 2b presents the ambient temperature and it can be seen again that in Tampere as high temperatures as in Strasbourg can be reached.

Figure 2c shows that the wind speed is more stable in Tampere and stays the most of the time between  $2.5 \text{ m/s}$  to  $5 \text{ m/s}$ . In Strasbourg the wind speed is really low the most of the week getting the values below  $2.5 \text{ m/s}$  but also getting really high values, over  $5 \text{ m/s}$ , during some period of the week.

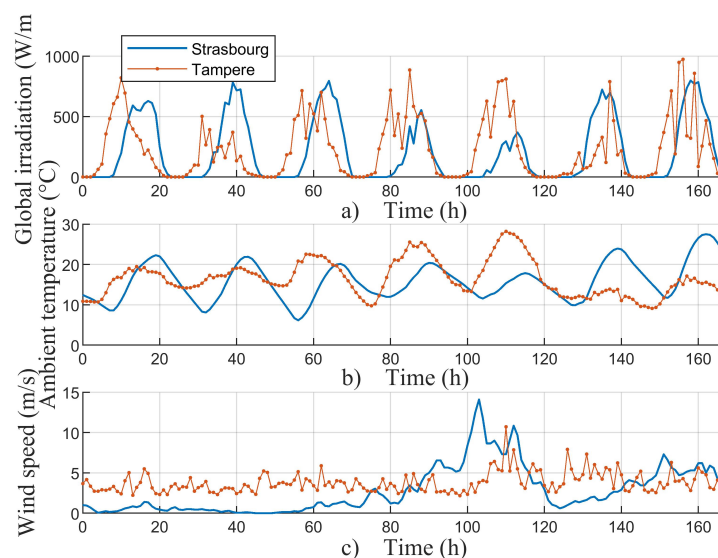


*Fig. 2. Climate conditions during a summer week in Tampere and Strasbourg: a) solar irradiation; b) ambient temperature; c) wind speed.*

Figure 3 shows the solar irradiation, ambient temperature and wind speed, respectively, during a winter week in Tampere and Strasbourg.

Figure 3a shows the solar irradiation at the end of December, which is the darkest time of the year. It can be seen that the solar irradiation in Tampere is almost non-existent and the PVT collector can produce neither electricity nor heat.

Figure 3b presents the ambient temperature, which reaches negative values in both Tampere and Strasbourg.

Figure 3c presents the wind speed, which is slightly slower in Tampere during the winter period than the summer period. On the other hand, in Strasbourg the wind speed is higher in winter than in summer period.

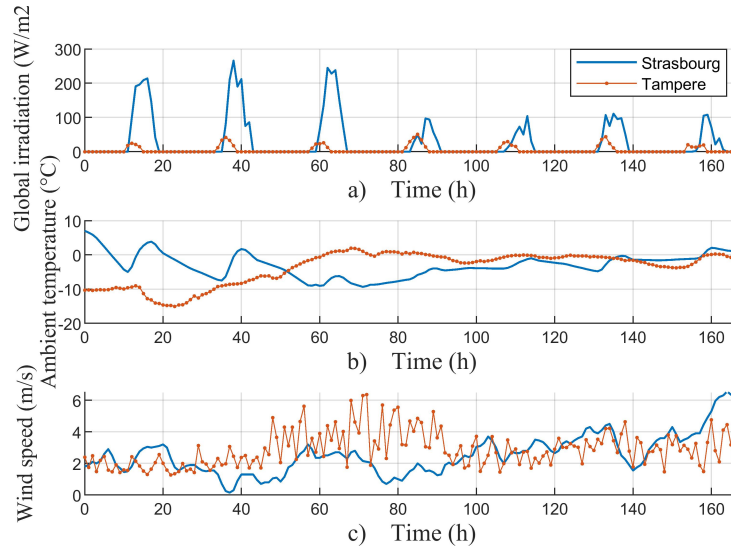


Fig. 3. Climate conditions during a winter week in Tampere and Strasbourg: a) solar irradiation; b) ambient temperature; c) wind speed.

Next the PVT collector model is built into the Matlab/Simulink and comparison of the PVT operation is conducted between Tampere and Strasbourg in terms of the energy and exergy analysis.

## 2.3. Mathematical model

In this paper, a simplified model of the PVT collector is presented. The mathematical model is implemented in Matlab/Simulink to assess the energy and exergy performance of the PVT collector under different climate conditions.

The PVT collector could be modelled a layer by layer to see the temperatures of each layer and the coolant fluid outlet temperature. However, in this paper, the study of the energy and exergy performance is conducted by looking at a simplified control volume in Fig. 4. The considered control volume composed of a cover glass, PV/absorber plate and a grid of tubes for the coolant fluid flow.

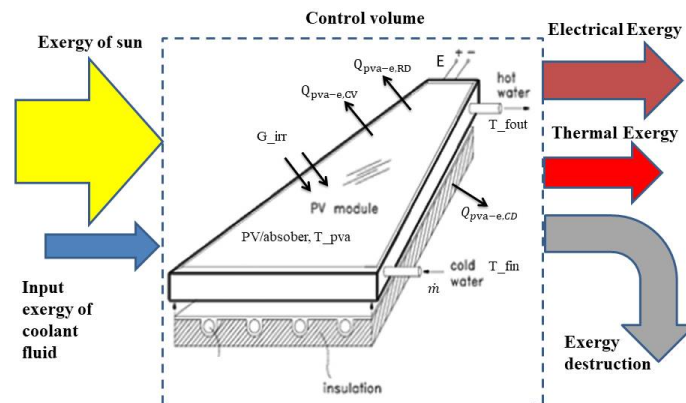


Fig. 4. The control volume and exergy flows of the PVT collector model



### 2.3.1 Numerical model for energy analysis

The energy analysis of the PVT collector is based on the First law of thermodynamics and energy performance of the system can be evaluated based on the analysis. The analysis takes into account the thermal and electrical efficiency of the PVT collector and thermal and electrical energy produced by the system during a certain time period.

First the energy balance equations are developed for the PV/absorber plate and for the coolant fluid. The PV/absorber layer consists of the cover glass and PV sandwich: PV glass, EVA layers, Si cell, tedlar, adhesive and absorber.

The equations are based on the variation of internal energy in a physical body:

$$Mc \frac{dT}{dt} = \frac{dU}{dt} \quad (1)$$

The energy balance for the **PV/absorber layer “pva”** considers on the right hand side the heat losses to the environment ( $Q_{losses}$ ), the useful heat transferred to the coolant circulating in the tube ( $Q_{pva-f}$ ), the heat absorbed by the glass ( $Q_g$ ) and PV/absorber layer ( $Q_{pva}$ ) and electricity production ( $E$ ). On the other hand, the heat losses to the environment consist of following terms: forced convective heat transfer due to wind ( $Q_{pva-e,CV}$ ), radiative losses ( $Q_{pva-e,RD}$ ) and conductive heat transfer through the insulation ( $Q_{pva-e,CD}$ ).

$$\begin{aligned} M_{pva} c_{pv} \frac{dT_{pva}}{dt} &= Q_{losses} + Q_{pva-f} + Q_g + Q_{pva} - E = \\ &= Q_{pva-e,CV} + Q_{pva-e,RD} + Q_{pva-e,CD} + Q_{pva-f} + Q_{pva} - E = \\ &= h_{pva-e,CV} A_{pva} (T_e - T_{pva}) + h_{pva-a,RD} A_{pva} (T_{sky} - T_{pva}) + h_{pva-e,CD} A_{pva} (T_e - \\ &T_{pva}) + h_{pva-f} A_{pva} (T_f - T_{pva}) + A_g \alpha_g G_{irr} + A_{pva} (\alpha \tau)_{pva} G_{irr} (1 - \eta_{EL}(T)) \end{aligned} \quad (2)$$

The heat transfer coefficient of forced convection ( $h_{pva-e,CV}$ ) is expressed through the correlation proposed by [11] and is widely used for numerical PVT models. The correlation covers the wind speed from 0 to 10 m/s.

$$h_{pva-e,CV} = \begin{cases} 5.7 + 3.8v_w, & \text{for } v_w < \frac{5m}{s} \\ 6.47 + v_w^{0.78} & \text{for } v_w > \frac{5m}{s} \end{cases} \quad (3)$$

The heat transfer coefficient of the radiative heat loss ( $h_{pva-e,RD}$ ) is calculated based on the emissivity of PV ( $\epsilon_{pv}$ ), the Stefan-Boltzmann constant ( $\sigma = 5.67 \times 10^{-8} \text{ W} \cdot \text{m}^{-2} \cdot \text{K}^{-4}$ ) and the equivalent radiative temperature of the sky ( $T_{sky}$ ). The temperature of the sky can be calculated as a linear function of the ambient temperature and the sky cloud coverage in octaves ( $N$ ) [2]. If clear sky conditions are assumed or there is no data available on the cloud coverage, Eq. (5) can be further simplified to Eq. (6), with less than 1% effect on the thermal and electrical output of the system [7,8].

$$h_{pva-e,RD} = \epsilon_g \sigma (T_g^2 + T_{sky}^2) (T_g + T_{sky}) \quad (4)$$

$$T_{sky} = 0.0552 T_e^{1.5} + 2.652 N \quad (5)$$

$$T_{sky} = 0.0552 T_e^{1.5} \quad (6)$$

The conductive heat transfer coefficient through the insulation ( $h_{pva-e,CD}$ ) to the environment is:

$$\frac{1}{h_{pva-e,CD}} = \frac{H_{insulation}}{k_{insulation}} \quad (7)$$

The heat transfer coefficient of the coolant fluid depends as follows on the type of the flow (laminar or turbulent) [12].

$$h_{a-f} = \begin{cases} 4.36 \frac{k_f}{D_H}, & \text{for } Re < 2300 \\ 0.023 \frac{k_f}{D_H} Re^{0.8} Pr^{0.4} & \text{for } Re > 2300 \\ 2 \frac{k_f}{D_H}, & \text{for } \dot{m} = 0 \text{ kg/s} \end{cases} \quad (8)$$

In order to take into account that the solar radiation comes to the PV/absorber layer through the glass layer the term  $(\alpha\tau)_{pva}$  in Eq. (2) is the effective product between glazing transmittance and plate absorptance. The term is calculated through the relation:

$$(\alpha\tau)_{pva} = \frac{\tau_g \alpha_{pv}}{1 - (1 - \alpha_{pv}) \rho_{gd}} \quad (9)$$

The PV converts a fraction of the solar radiation into the electricity. However, this also increases the operation temperature  $T_{pva}$ , which causes a reduction of the electrical efficiency of the PV. Due to this the electrical efficiency of the PV depends linearly on the temperature  $T_{pva}$ , the temperature coefficient  $\beta_{PV}$  and on the efficiency at standard conditions  $T_{ref}$ . The efficiency is calculated according to the following relation used widely in the literature [3, 5, 7, 8]:

$$\eta_{EL(T)} = \eta_{STC} [1 - \beta_{PV}(T_{pva} - T_{ref})] \quad (10)$$

Above mentioned relation do not take into account a maximum power point tracking. Due to this PV panel output is independent from the electricity demand profile and a direct grid-connection can be assumed.

The energy balance for **the coolant fluid “f”** considers on the right hand side the

$$M_f C_f \frac{dT_f}{dt} = Q_{f-pva} + Q_f = h_{pva-f} \frac{\pi DL}{2} (T_{pva} - T_f) + \dot{m}_f (T_{f,in} - T_{f,out}) \quad (11)$$

The heat transfer coefficient of the coolant fluid ( $h_{pva-f}$ ) is calculated in Eq. (8).  $T_f$  is the mean temperature of the fluid. The mass flow rate of the fluid in the channels is  $\dot{m}$  (kg/s) and  $T_{fin}$  and  $T_{fout}$  are the inlet and outlet temperatures of the fluid, respectively.

The Equation (2) and (11) are implemented to the Matlab/Simulink in order to assess energy performance of the PVT collector in different climate conditions. The following thermal, electrical and overall efficiencies can be calculated:

$$\eta_{EL} = \frac{P_{EL}}{A_{pva} G_{irr}} \quad (12)$$

$$\eta_{TH} = \frac{\dot{m}_f (T_{f,out} - T_{f,in})}{A_{pva} G_{irr}} \quad (13)$$

$$\eta = \frac{\dot{m}_f (T_{f,out} - T_{f,in}) + P_{EL}}{A G_{irr}} \quad (14)$$

### 2.3.2. Numerical model for exergy analysis

Compared to energy analysis the exergy analysis is based on the Second Law of Thermodynamics, which defines that entropy is always increasing and a system goes towards equilibrium with its environment. Due to this, the exergy analysis measures the quality of produced energy in terms of mechanical work.

The exergy balance of the system can be expressed as follows:

$$\sum Ex_{in} - \sum (Ex_{th} + Ex_{el}) = \sum Ex_d \quad (15)$$

In the case of PVT collector the exergy flow to the system  $Ex_{in}$  comes from the solar irradiation. However, solar irradiation is not seen as pure exergy and due to this a conversion coefficient is included in the calculation of the PVT incoming exergy [10]:

$$Ex_{in} = A_{pva} N_c G_{irr} \left( 1 - \frac{4}{3} \frac{T_0}{T_{sol}} + \frac{1}{3} \left( \frac{T_0}{T_{sol}} \right)^4 \right) \quad (16)$$

In Eq. (16)  $T_{sol}$  is the solar temperature and  $T_0$  is the reference temperature which according to the literature should be a constant, for example,  $T_0 = 20^\circ\text{C}$ ,  $T_0 = 25^\circ\text{C}$  or the minimum temperature of the month. In this study  $T_0 = 20^\circ\text{C}$  is used.  $N_c$  is a number of the collectors.

Electric energy is seen as pure exergy but the exergy content of thermal energy depends on the temperature at which the heat is made available. In the model the exergy of thermal ( $Ex_{th}$ ) and electric ( $Ex_{el}$ ) energy are calculated as follows respectively [10]:

$$Ex_{th} = \dot{m} c_f \left[ (T_{out} - T_{in}) - T_0 \ln \frac{T_{out}}{T_{in}} \right] \quad (17)$$

$$Ex_{el} = \eta_{pv} G_{irr} A_{pv} \quad (18)$$

The exergy efficiency is broken into thermal ( $\xi_{th}$ ) and electrical exergy ( $\xi_{el}$ ) efficiencies in order to assess the quality of the different energy components. By Eqs. (19, 20, 21) the both thermal ( $\xi_{th}$ ) and electrical exergy ( $\xi_{el}$ ) efficiencies and the overall exergy efficiency ( $\xi$ ) of the PVT collector can be calculated as follows:

$$\xi_{th} = \frac{Ex_{th}}{Ex_{in}} \quad (19)$$

$$\xi_{el} = \frac{Ex_{el}}{Ex_{in}} \quad (20)$$

$$\xi_{el} = \frac{Ex_{el} + Ex_{th}}{Ex_{in}} \quad (21)$$

### 3. Results and discussion

First, the hourly simulations were run with the PVT collector model during selected summer and winter weeks. In order to see a big picture of the PVT collector operation, the yearly simulations were conducted. The summer week was selected to present a typical good summer week in Tampere and Strasbourg to assess production ability between the different locations. Due to the northern location of Tampere, the selected summer week was between 24.-30.6. and in Strasbourg between 4.-10.8. The winter week was in both cases between 23.-29.12.

Figure 5 shows the exergy of the produced electrical power. Due to the fact that electric power is pure exergy Fig. 5 shows also produced electrical power during the summer and winter weeks. The overall electrical exergy efficiency over the summer and winter week was 13.08% and 14.95%, respectively, in Tampere, and 13.03% and 14.62%, respectively, in Strasbourg. The efficiencies were slightly higher in Tampere due to the cooler operating conditions.

On the other hand, the overall thermal exergy efficiency during the summer week was 0.54% in Tampere and 0.69% in Strasbourg. The results are reasonable when compared to the exergy analysis results in [10]. In these results, the thermal exergy efficiency varies between 0.5-1.23 per cent when pure water is used as a coolant fluid. During the winter week, thermal energy production did not

exist because the solar irradiation and ambient temperature were significantly lower than during the summer week. The overall exergy efficiency was 13.62% and 14.95% over the summer and winter weeks, respectively, in Tampere. In Strasbourg, this was 13.71% and 14.62%, respectively.

The thermal exergy efficiency is in both locations significantly lower than the thermal efficiency which reaches its maximum value around 60% during the warmest day of the summer week. This means that the PVT collector can convert the available solar energy well into useful heat but it happens really close to the reference ambient temperature and its ability to work is really low. The reference ambient temperature was set to be  $T_0 = 20\text{ °C}$  in this study. In the literature, this value is recommended to be a constant and there are few different approaches to select the reference temperature for the exergy analysis [3]. The other approach is to select the minimum outdoor temperature registered during any given months [3].

Figure 6 shows the thermal exergy efficiency and coolant outlet temperature in Strasbourg and Tampere during the summer week. The thermal exergy efficiency got the lowest values in both locations when the outlet temperature was close to the reference ambient temperature of  $20\text{ °C}$ . The outlet temperature varied mainly between  $25\text{--}35\text{ °C}$ . The better comparison between two different locations requires setting a climate depending reference ambient temperature.

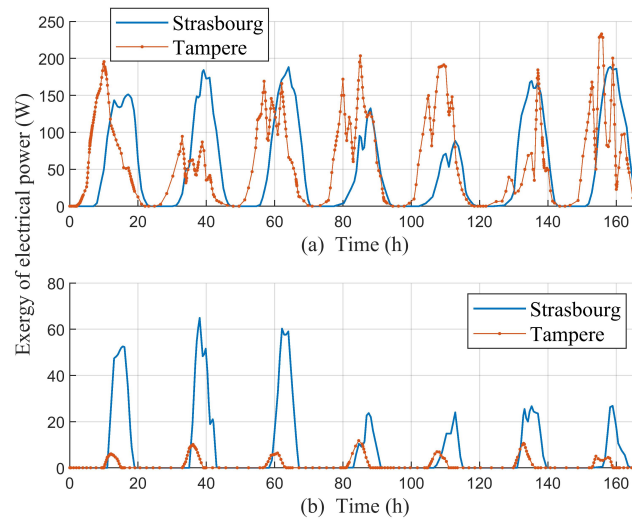


*Fig. 5. Exergy of electrical power during: a) summer week; b) winter week*

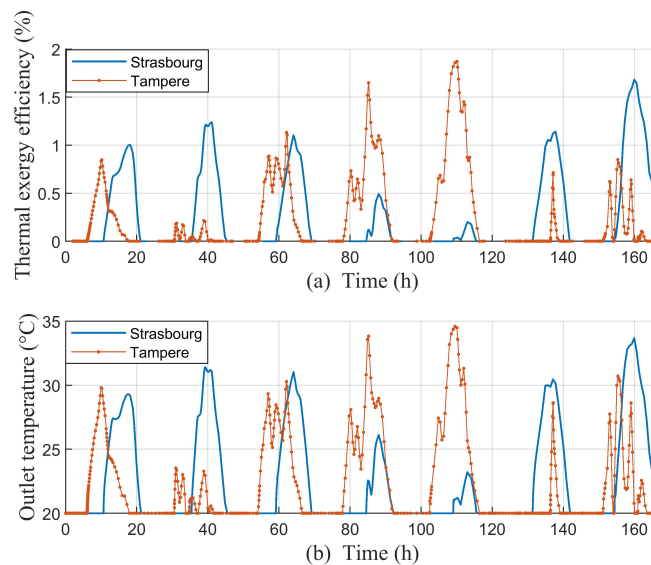


*Fig. 6. Strasbourg and Tampere during the summer week: (a) Thermal exergy efficiency, (b) outlet temperature*

The electrical exergy efficiency is influenced by the operating temperature of the PVT collector. In Fig. 7 can be seen how the electrical exergy efficiency decreased when the PVT collector surface and coolant fluid outlet temperatures increased, and vice versa. Due to this conflicting nature of the PVT operation, the multi-objective optimization is required to find optimal design and operation variables that lead to a trade-off solution for the thermal and electrical efficiencies.

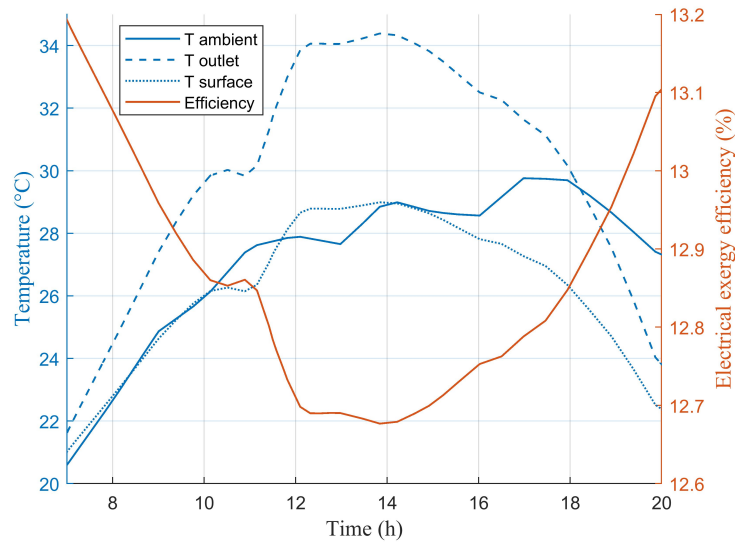


Fig. 7. The electrical exergy efficiency, PVT surface, fluid outlet and ambient temperature during a summer day.

In Fig. 8 and 9 is shown yearly exergy of electrical and thermal power. The thermal production of the PVT collector was controlled in the model by the inlet fluid temperature. If the outlet temperature of the coolant fluid decreased below the inlet temperature, the coolant circulation was stopped.

Figure 8 shows that the PVT collector was able to produce electricity over a year in Strasbourg and Tampere. However, in Tampere there was a clear reduction in the production compared to Strasbourg during the last months of the year and at the beginning of the year. On the other hand, the electricity production was more intensive in Tampere during the summer months than in Strasbourg.

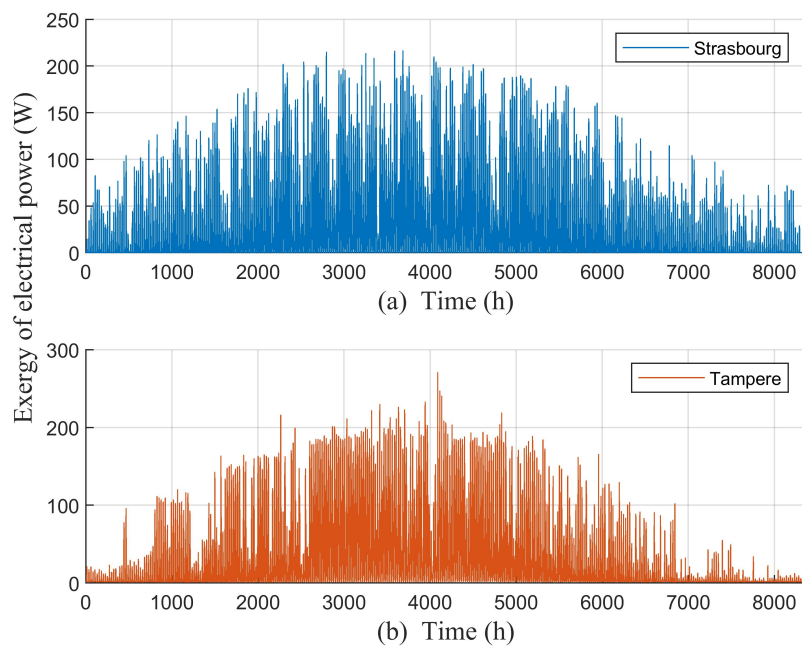


Fig. 8. Exergy of electrical power during a year: a) Strasbourg; b) Tampere

Figure 9 presents the annual thermal exergy production. Thermal exergy was not produced during the winter months due to colder ambient temperatures and lower or non-existent solar irradiation. In Strasbourg, the period to produce thermal exergy was longer than in Tampere. However, the production was again more intensive in Tampere.

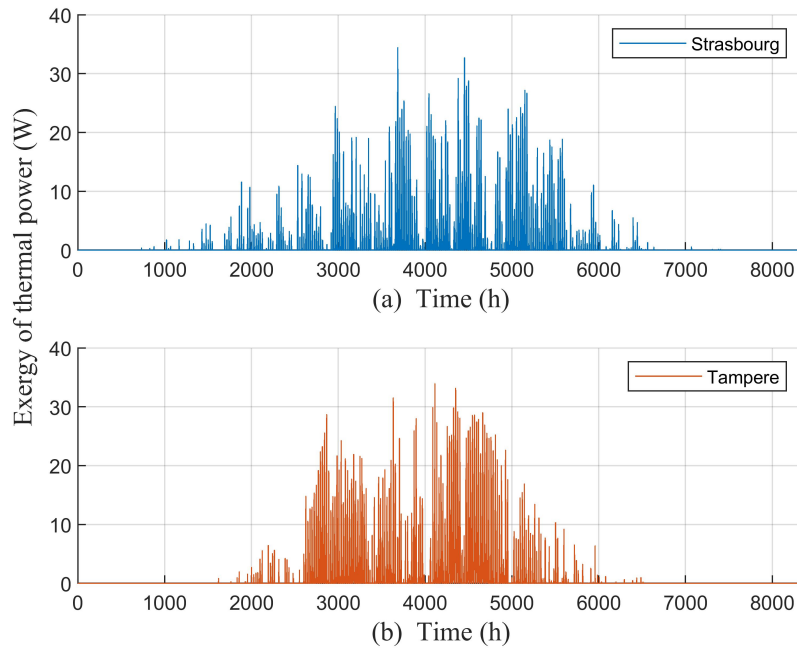


Fig. 9. Exergy of thermal power during a year: a) Strasbourg; b) Tampere

Table 2 summarizes the annual energy ( $E$ ) and exergy ( $Ex$ ) production and the corresponding efficiencies. The yearly solar gain was 2161.3 kWh in Strasbourg and 2069.2 kWh in Tampere. The yearly results show the same fact than the weekly results that the produced thermal energy results in really low thermal exergy efficiency, which indicates low quality of the energy in terms of mechanical work.

Table 2. Annual energy and exergy production and efficiencies

|                   | Stras $E_{th}$<br>[kWh] | Tam $E_{th}$<br>[kWh] | Stras $E_{el}$<br>[kWh] | Tam $E_{el}$<br>[kWh] | Stras<br>$Ex_{th}$<br>[kWh] | Tam<br>$Ex_{th}$<br>[kWh] | Stras<br>$Ex_{el}$<br>[kWh] | Tam $Ex_{el}$<br>[kWh] |
|-------------------|-------------------------|-----------------------|-------------------------|-----------------------|-----------------------------|---------------------------|-----------------------------|------------------------|
|                   | 718.35                  | 682.56                | 266.55                  | 257.15                | 9.61                        | 9.79                      | 266.55                      | 257.15                 |
| Efficiency<br>[%] | 33.24                   | 33.1                  | 12.33                   | 12.43                 | 0.48                        | 0.51                      | 13.23                       | 13.33                  |

The sensitivity analysis was conducted to analyse how sensitive thermal and electrical exergy efficiencies were for a change in coolant inlet temperature and mass flow rate. The results are shown in Fig. 10. The steepness of the slope indicates how strongly a variable influences to the efficiency. In Fig. 10 can be seen that the inlet temperature influenced the most to the both efficiencies. However, the mass flow rate had also a strong impact on the efficiencies.

First, the mass flow was varied  $\pm 20$  and  $40\%$  from the base case. The smaller mass flow rate resulted in the higher thermal exergy efficiency. However, after a certain point the efficiency was not increased anymore but decreased. The higher mass flow rate decreased thermal exergy efficiency due to higher amount of coolant passing the collector. Increasing the mass flow rate increased the electrical exergy efficiency first strongly and then the rise levelled off but still increased. The increase was resulted in by the stronger cooling effect on the PV panel. Next, the inlet water temperature was varied  $\pm 20$  and  $40\%$  from the base case. The increase in the inlet temperature resulted in a strong increase in the thermal exergy efficiency due to the higher outlet



temperature. However, the increased inlet temperature decreased the electrical exergy efficiency due to the higher operating temperature of the collector and the reduced cooling effect on the PV panel.

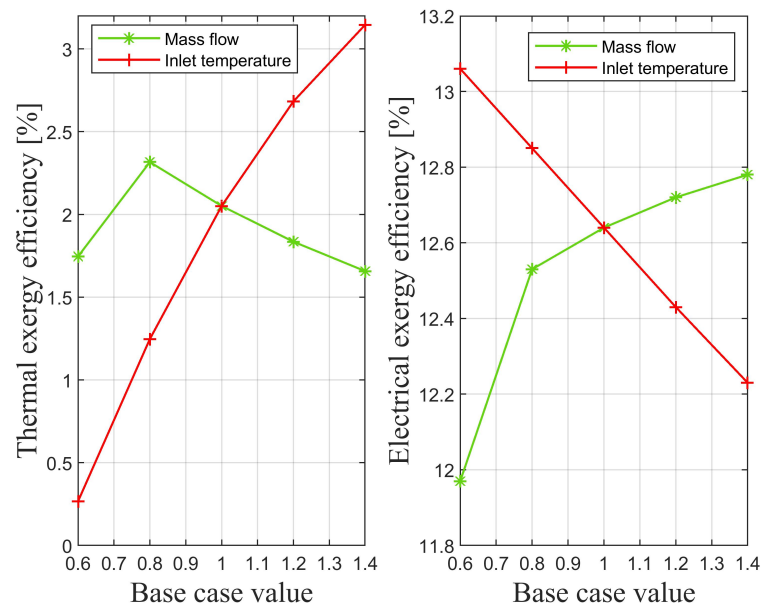


Fig. 10. The sensitivity analysis: a) Thermal exergy efficiency; b) Electrical exergy efficiency

The results of the sensitivity analysis should be taken into account when optimizing the PVT collector operation parameters in terms of the thermal and electrical exergy efficiencies.

## 4. Conclusion

In this study, the mathematical model of the water-cooled PVT collector was implemented into Matlab/Simulink to simulate the operation of the PVT collector under two different European climate conditions in Tampere, Finland and Strasbourg, France. The energy performance of the PVT collector operation was evaluated mainly according to the exergy analysis. Last, the sensitivity analysis was performed to see how sensitive the PVT operation is for the coolant mass flow rate and inlet temperature.

Compared to the energy analysis, the exergy analysis revealed that the PVT collector can convert the available solar energy well into useful heat but its quality in terms of mechanical work is really low. This happens when the heat is produced close to the reference ambient temperature.

The energy analysis showed that the yearly thermal energy production was 5.2% higher in Strasbourg than in Tampere. However, the thermal exergy production was 1.87% higher in Tampere than in Strasbourg. This result shows that the produced thermal energy had a higher quality in terms of mechanical work in the northern than southern location.

The sensitivity analysis revealed that the coolant mass flow rate and inlet temperature had a strong influence on the thermal and electrical exergy efficiencies. If the mass flow rate is decreased and the inlet temperature increased the thermal exergy efficiency is enhanced and electrical exergy efficiency decreased, and vice versa. However, in terms of the overall exergy efficiency the increase is reached if the mass flow rate is low and inlet temperature high. The lower coolant mass flow has a better advantage in PVT building applications due to lower pumping power requirements and lighter piping.

In future work, the multi-objective optimization should be conducted to find the optimal coolant mass flow and inlet temperature that maximize the thermal and electrical exergy efficiencies in their conflicting nature. The overall exergy efficiency can be increased more if the thermal exergy efficiency is increased. Due to this the optimization could include also reasonable design variables, such as air gap and insulation thickness. Additionally, the mathematical model of the PVT collector

should be improved with separated layers, such as cover glass, PV panel, absorber plate and water tube to analyse better thermal behaviour of the collector. The improved model should be validated based on the literature.

The exergy analysis and comparison between two different climate conditions should be enhanced by taking into account the monthly average temperatures as a reference ambient temperature and calculate monthly results.

For future research, it would be interesting to couple the PVT collector with thermal and electrical storages, and energy demand profiles.

## Acknowledgments

The authors would like to thank Interreg V Rhin supérieur for their support and funding of this research.

## References

- [1] Barbu M., Darie G., Siroux M., Analysis of a residential photovoltaic-thermal (PVT) system in two similar climate conditions. *Energies*, 2019.
- [2] Aste N., Leonforte F., Del Pero C., Design, modelling and performance monitoring of a photovoltaic-thermal (PVT) water collector. *Solar Energy*, vol 112, pp. 85-99, 2015.
- [3] Evola G., Marletta L., Exergy and thermoeconomic optimization of a water-cooled glazed hybrid photovoltaic/thermal (PVT) collector. *Solar Energy*, vol 107, p. 12-25, 2014.
- [4] Da Silva R.M., Fernandes J.L.M., Hybrid photovoltaic/thermal (PV/T) solar systems simulation with Simulink/Matlab. *Solar Energy*, vol. 84, p. 1985-1996, 2010.
- [5] Dubey S., Tiwari G.N., Analysis of PV/T flat plate water collectors connected in series. *Solar Energy*, vol. 83, p. 1485-1498, 2009.
- [6] Herrando M., Ramos A., Freeman J., Zabalza I., Markides C., Technoeconomic modelling and optimisation of solar combined heat and power systems based on flat-box PVT collectors for domestic applications. *Energy Conversion and Management*, vol. 175, p. 67-85, 2018.
- [7] Guarracino I., Mellor A., Ekins-Daukes NJ., Markides CN., Dynamic coupled thermal-and-electrical modelling of sheet-and-tube hybrid photovoltaic/thermal (PVT) collectors. *Appl. Therm. Eng.*, vol. 101, p. 778–795, 2016.
- [8] Touafek K., Khelifa A., Adouane M., Theoretical and experimental study of sheet and tubes hybrid PVT collector. *Energy Convers. Manag.*, vol. 80, p. 71–77, 2014.
- [9] Feidt M., Costea M., Energy and exergy analysis and optimization of combined heat and power systems. Comparison of various systems. *Energies.*, vol. 5, p. 3701-3733, 2012.
- [10] Farzanehnia A., Sardarabadi M., Exergy in Photovoltaic/Thermal Nanofluid-Based Collector Systems. In: Aziz M., editors. *Exergy and Its Application - Toward Green Energy Production and Sustainable Environment*. IntechOpen. 2019. p. 1-14.
- [11] McAdams WH, Heat transmission. 3rd ed. New York: McGraw-Hill; 1954.
- [12] Incropera F, Fundamentals of heat and mass transfer. John Wiley and Sons. 2011.